Published in final edited form as:
J Cardiovasc Transl Res. 2011 June ; 4(3): 363–372. doi:10.1007/s12265-011-9265-3.

Constitutive HIF-1α Expression Blunts the Beneficial Effects of Cardiosphere-Derived Cell Therapy in the Heart by Altering Paracrine Factor Balance

Michael Bonios, **Connie Yachan Chang**, **John Terrovitis**, **Aurelio Pinheiro**, **Andreas Barth**, **Peihong Dong**, **Miguel Santaularia**, **D. Brian Foster**, **Venu Raman**, **Theodore P. Abraham**, and **Maria Roselle Abraham**
Johns Hopkins University, 720 Rutland Ave, Ross 871, Baltimore, MD 21205, USA

Abstract

Hypoxia-inducible factor-1alpha (HIF-1α) expression promotes angiogenesis and can influence stem cell engraftment. We investigated the effect of stable over-expression of constitutively active HIF-1α on cardiosphere-derived cell (CDC) engraftment and left ventricular function. CDCs were transduced with a lentivirus expressing a constitutively active mutant of human HIF-1α (LVHIF-1α). Two million male rat CDCs were injected into the infarct following ligation of the mid-LAD in female syngeneic rats. Left ventricular ejection fraction (EF) and circumferential strain were measured by echocardiography at 1 and 4 weeks post-MI in the following groups: PBS group (*n*=7), CELL group (*n*=7), and CELL-HIF group (*n*=7). HIF-1α, VEGF, endothelin-1 expression, and CDC engraftment were measured by quantitative PCR. At 30 days, EF was unchanged in the CELL-HIF group (*p*=NS), increased in the CELL group (*p*=0.025), and decreased in the PBS group (*p*=0.021), but engraftment was similar (2.4%±3.3% vs 1.7%±0.8%, *p*=NS). Mean circumferential strain of the infarcted region was unchanged in the CELL-HIF group, but improved in the CELL group (*p*=0.02). Endothelin-1 and VEGF expression were higher in HIF-CDCs exposed to hypoxia, compared with non-transduced CDCs. HIF-1α expression in CDCs blunted the beneficial functional effects of CDC transplantation, suggesting that paracrine factor balance may play an important role in cardiac regeneration.

Keywords

Constitutively active HIF-1α; Paracrine factor balance; Cardiac regeneration; Cardiosphere-derived cells; Animal models of human disease; Echocardiography; myocardial infarction

Introduction

Stem cell therapy has emerged as a novel therapeutic strategy in patients with ischemic cardiomyopathy [1]. Cardiosphere-derived cell (CDC) therapy is currently in clinical trials (CADUCEUS at www.clinicaltrials.gov). Studies in animal models confirm that CDCs can engraft, but improvement in ejection fraction is not consistent and engraftment is low [2]. Experimental work suggests that cell transplantation in the post-MI period may paradoxically promote engraftment suggesting that the microenvironment plays an important

M. R. Abraham mabraha3@jhmi.edu .
Michael Bonios and Connie Y. Chang contributed equally to the work.

Disclosures None

role [3]. A possible mechanism underlying this effect is secretion of growth factors, cytokines and activation of transcription factors like HIF-1α, a master-regulator of oxygen homeostasis, in infarcted myocardium. HIF is composed of an alpha subunit (HIF-1α or HIF-2α) and a β subunit (aryl hydrocarbon receptor nuclear translocator (ARNT)) [4]. HIF-1α is labile during normoxia, but stabilized by hypoxia, enabling dimerization with ARNT to induce genes involved in a variety of processes, including paracrine factor secretion, glucose uptake, metabolism, erythropoiesis, angiogenesis, vasculogenesis, regulation of vascular tone, cell proliferation as well as stem cell homing, adhesion, migration, and survival [5–11]. Despite stabilization of the alpha subunit by hypoxia, HIF-1α protein levels peak within 24 h after ischemia and then progressively decline over the next 2–3 days [12, 13], prompting the use of *constitutively active* HIF-1α mutants in promoting angiogenesis [14, 15]. Hence, we hypothesized that constitutive HIF-1α over-expression in CDCs would increase CDC engraftment and the functional effects of CDC transplantation in the heart. Here, we used a *constitutively active* mutant of human HIF-1a (kind gift from Dr. Gregg Semenza, Johns Hopkins University) that contains a deletion (residues, 392–520) [16] and two missense mutations (Pro567Thr and Pro658Gln) which prevent its degradation [14, 15]. Transduction of CDCs with a lentivirus expressing constitutively active human HIF-1α increased VEGF expression, but not tube formation (angiogenesis) under normoxia. Following transplantation post-MI, left ventricular ejection fraction (EF) and myocardial strain in the infarct/peri-infarct region were unchanged in the animals receiving HIF-transduced CDCs, increased in the control group that received non-transduced CDCs and decreased in the placebo group that received PBS injections. Quantitative PCR revealed higher VEGF and endothelin-1 (ET-1) expression in HIF-transduced CDCs following exposure to hypoxia, when compared with control, non-transduced CDCs. Lack of functional benefit in the group receiving HIF-transduced cells is probably mediated by paracrine factors like endothelin-1 which promote adverse remodeling and negate the beneficial effects of factors like VEGF [17]. Our results suggest that *paracrine factor balance* may play an important role in determining the functional benefits following cell transplantation.

Methods

All animal procedures were conducted in accordance with humane animal care standards outlined in the NIH Guide for the Care and Use of Experimental Animals and were approved by the Johns Hopkins University Animal Care and Use Committee.

Cardiosphere-Derived Cell Isolation

Hearts were explanted from 3-month-old male WK rats, under sterile conditions. Myocardial tissue was cut into pieces (explants) and cultured in complete explant medium or CEM (Iscove's modified Dulbecco medium/IMDM containing 20% heat-inactivated fetal calf serum, penicillin G, streptomycin, L-glutamine and 0.1 mmol/L 2-mercaptoethanol) on fibronectin-coated dishes at 37°C and 5% CO_2. After a period ranging from 4 to 7 days, a layer of fibroblast-like cells arises from adherent explants over which small, round, phase-bright cells migrate. These cells were collected and seeded at ~ 0.5 – 10^5cells on poly-D-lysine-coated plates in cardiosphere growth medium or CGM (35% IMDM/65% DMEM-Ham's F-12 (GIBCO), 2% B27 (GIBCO), 0.1 mmol/L 2-mercaptoethanol (GIBCO), 10 ng/mL EGF (RD Systems), 20 ng/mL bFGF (PeproTech), and 4 ng/mL cardiotrophin-1 (RD Systems), 1 U/mL thrombin (Sigma), 100 U/mL penicillin G, 100 U/mL streptomycin, and 2 mmol/L L-glutamine), to yield spherical cell clusters called cardiospheres, which grow in suspension. This process was repeated twice at 5–7-day intervals from the same explant. Cardiospheres were harvested and plated on fibronectin-coated flasks in CEM to generate monolayers that we call cardiosphere-derived cells or CDCs. CDCs obtained from the

second harvest were passaged twice and frozen for future use. For in vivo and in vitro experiments, these CDCs were thawed and expanded for two more passages prior to use.

Lentivirus Production

A third-generation lentiviral vector system was used to label CDCs. Expression of the transgene was driven by the constitutively active promoter CMV. Constitutively active HIF-1α (a kind gift from Dr. Gregg Semenza, Johns Hopkins University) is sub-cloned from the AdCA5 plasmid [14] into the vector, pRRLsin18.cPPT.CMV.eGFP. Wpre in place of expressing green fluorescent protein (eGFP). The constitutively active HIF-1α, generated by mutagenesis in the wild-type HIF-1α promotes stabilization of the protein even in the absence of hypoxia.

Viral vectors were produced by Lipofectamine 2000 transfection of four lentiviral vector plasmids into HEK293 cells. [18] Vector-containing supernatant was collected 48 and 72 h after transfection, filtered (0.45 μm, cellulose acetate) and concentrated by ultrafiltration (100,000 MWCO). Viral titer was assigned on concentrated supernatant by HIV-1 p24 ELISA (Cell Biolabs). Rat CDCs (P3) were transduced at a multiplicity of infection of 20, expanded for two passages and used for in vitro and in vivo experiments.

Expression Analysis by Quantitative PCR

Expression of human and rat HIF-1α, and the downstream target genes VEGF and endothelin-1 was tested by quantitative real-time PCR, during normoxia and hypoxia. RNA was isolated using the AllPrep DNA/RNA mini kit (Quigen), as per manufacturer's protocol.

Cells were transferred to a modular Incubator chamber (Billups-Rothenberg, Del Mar, CA) containing 1%O_2, 5%CO_2, and 94% N_2 for all hypoxia experiments.

For the measurement of human-specific HIF, rat-specific HIF and rat-specific VEGF mRNA levels before and after 24 h of hypoxia, commercially available primers and probes were used (TaqMan® Gene expression assays, Applied Biosystems). The 18S rRNA of each sample was quantified [19] and used as calibrator (TaqMan Ribosomal control, Applied Biosystems). Real-time PCR was performed in an ABI PRISM 7700 instrument and each sample was tested in triplicate. Copy numbers of all target genes were calculated using standard curves constructed separately for each target. For each sample, the mRNA levels of the genes of interest were calibrated according to the corresponding 18S rRNA quantity and then normalized according to the control sample. Results are expressed as fold increase over control.

For the detection of endothelin-1, cells were exposed to hypoxia for 70 h in CEM (containing 2% FBS and 30 mg/dL glucose) in order to simulate the in vivo infarct environment. RNA was extracted immediately after removing the cells from the Modular Incubator chamber (Billups-Rothenberg, Del Mar, CA). Subsequently, 200 ng RNA from each sample was reverse transcribed into cDNA using qScript cDNA Synthesis Kit (Quanta Biosciences) according to manufacturer's protocol. Quantitative PCR for entdothelin-1 was performed using the BioRAD iQ5 Multicolor real-time PCR Detection system and B-R SYBR green supermix for iQ (Quanta Biosciences). Each reaction contained: 10 ul of B-R SYBR green supermix, 1 ul cDNA, 1 uM forward primer (5′-TACAGAGACCAGAAGTTGATAC-3′), 1 uM reverse primer (5′TAGAAGCCGGACAGATGTTC-3′), and DNase–RNase-free water to a final volume of 20 ul. Amplification of 18srRNA (TaqMan Ribosomal control, Applied Biosystems) of each sample was used for normalizing gene expression values. Amplification was placed in a MicroAmp Fast 96-well reaction plate (Applied Biosystems). The primers amplified a 154-

bp region [20]. ΔC_t=C_t (non-transduced CDCs or HIF-1α-transduced CDCs)–C_t (18S rRNA). Fold difference was calculated by the formula $2^{-\Delta\Delta C_t}$, where $\Delta\Delta C_t$=ΔC_t (HIF-1α-transduced CDCs)–ΔC_t (non-transduced CDCs).

We performed Western blots for endothelin-1 in order to confirm results of qPCR, but the results were inconclusive due to problems with antibody (Santa Cruz) specificity.

Quantification of Engraftment by Quantitative PCR

Animals from the CELL and HIF-CELL groups were sacrificed 4 weeks post-MI/transplantation, hearts were explanted, weighed and homogenized. We injected cells harvested from male rats into female recipients, an experimental design that allowed us to use the male specific SRY gene, located on the Y chromosome, as a target for the real-time PCR [21]. Since there is only one copy of the SRY gene per cell, the number of copies of the SRY gene (determined by real-time PCR) in the recipient heart corresponds to the number of transplanted cells.

Genomic DNA was isolated from aliquots of the homogenate corresponding to 12.5 mg of myocardial tissue, according to the manufacturer's instructions (Qiagen). Real-time PCR was performed using the TaqMan® chemistry (Applied Biosystems), with the rat SRY gene as target (forward primer: 5′-GGA GAG AGG CAC AAG TTG GC-3′, reverse primer: 5′-TCC CAG CTG CTT GCT GAT C-3′, TaqMan probe: 6FAM CAA CAG AAT CCC AGC ATG CAG AAT TCA G TAMRA). For absolute quantification of gene copy number, a standard curve was constructed with samples derived from multiple log dilutions of genomic DNA isolated from male rat CDCs. All samples were spiked with 50 ng of female genomic DNA to control for any effects this may have on reaction efficiency in the actual samples. The copy number of the SRY gene at each point of the standard curve is calculated based on the amount of DNA in each sample and total mass of the rat genome per diploid cell. (http:www.cbs.dtu.dk/databases/DOGS/index.html). All samples were tested in triplicate. For each reaction, 50 ng of template DNA was used. Real-time PCR was performed in an ABI PRISM 7700 instrument. The result from each reaction, i.e., copies of the SRY gene in 50 ng of genomic DNA, was expressed as the number of engrafted cells/heart, by first calculating the copy number of the SRY gene in the total amount of DNA corresponding to 12.5 mg of myocardium and then extrapolating to the total weight of each heart.

Assessment of CDC Viability and Proliferation Under Normoxia and Hypoxia

A WST-8-based (Cell Counting Kit-8, Dojindo Molecular Technologies, MD, USA) colorimetric assay was initially used to quantify cell viability and proliferation under normoxia and hypoxia. The assay detects extracellular reduction of WST-8 by NADH produced in the mitochondria [22]. The assay was performed daily for 7 days on control and LVCAHif-1α-transduced rat CDCs during normoxia and following exposure to hypoxia for 48 h. CDCs were incubated with 10 μl of WST-8 tetrazolium salt for 2 h and absorbance was measured at 450 nm (Spectramax M2, Molecular Devices, Sunnyvale, CA, USA). The tetrazolium salt WST-8 is cleaved to form formazan by cellular mitochondrial dehydrogenase. The number of living cells is directly proportional to the amount of formazan dye which can only be produced by viable cells and generated by the activity of dehydrogenase. As a result, the higher the absorbance at 450 nm, the more metabolically active and viable the cells are. The results were expressed as: (absorbance on a specific day/absorbance measured at baseline) ×100%. Proliferation experiments were repeated two times, with each condition tested in triplicate.

Since WST-8 results depend on mitochondrial dehydrogenase activity which may be altered by hypoxia or HIF expression, 5-ethynyl-2′-deoxyuridine (EdU) incorporation was

measured by flow cytometry. Here, LVCAHif-1α-transduced and control CDCs were labeled with EdU (Invitrogen), an alkyne-conjugated nucleoside analog of thymidine. EdU is incorporated into DNA during active DNA synthesis and thus provides an estimate of the number of cells in the S-phase of the cell cycle. Cells were incubated with15 μM Edu for 12 h and then processed for EdU detection according to the manufacturer's protocol (Click-IT Flow Cytometry Assay kit; Invitrogen). For flow cytometry, all cells were also labeled with 7-aminoactinomycin D (7-AAD; 4 ug/ml; Invitrogen), a fluorescent marker for DNA for 30 min. After staining, cells were analyzed by flow cytometry using a FACSCalibur flow cytometer with CellQuest software (BD Biosciences, San Jose, California), based on 488 nm excitation with green emission filter (530/30 nm) and 7-AAD using 488 nm excitation and red emission filter (660/20 nm).

In Vitro Angiogenesis Assay

Angiogenic potential was assessed using a BD BioCoat Angiogenesis System (Becton-Dickinson, Franklin Lakes, NJ). We plated 1×10^4 cells (LVCAHif-1α-transduced and control CDCs) in triplicate in the 96-well plate in CEM containing 2.5% FBS. Human vascular endothelial cells (HUVEC) served as a positive control. Tube formation was monitored at 4 and 24 h under normoxia. Quantification of tube formation was performed using Image J (NIH) with the Neuron J plug-in to delineate the total tube length and the number of branch points. Tube formation was analyzed by manually measuring the total tube length in three different wells per sample. Measurements were taken in several random view-fields per well and the values were averaged.

Echocardiography

We performed echocardiograms at 2 time points, namely, 1 and 4 weeks post-MI. We chose the 1 week time point because of poor image quality early after MI due to presence of a left-sided pneumothorax.

Rats were anesthetized with 1.5% isoflurane (using a nose cone) for the duration of imaging; heart rate was monitored and the animals' body temperature was maintained at 37°C during image acquisition. We used a 14-MHz transducer coupled to a Vivid 7 echocardiography machine (GE Medical, Milwaukee, WI). Two dimensional long axis images were used for the measurement of ejection fraction (calculated as the difference between end-diastolic and end-systolic volumes normalized to end-diastolic volume, expressed as a percentage). Subsequently, an apical short-axis image (distal to the papillary muscle in order to include the infarcted area) and a basal image (at the level of the papillary muscles) were acquired. The adjustments of the sector width for this transducer resulted in a maximum frame rate of 90–100 frames/s. We calculated mean circumferential strain which was defined as the average strain of all segments in a particular short- axis view.

Circumferential Strain—We measured strain which is a sensitive indicator of regional and global cardiac function and has been extensively validated in experimental and human studies [23, 24]. We used circumferential strain for multiple reasons. Firstly, circumferential strain has been shown to be a more dynamic parameter and indicative of dyssynchrony in an experimental model [25]. Secondly, the feasibility and reproducibility of circumferential strain in small animals is superior to longitudinal and radial strain. Apical long axis views in rodents are challenging to obtain repeatedly, reducing the feasibility of longitudinal strain. Similarly, due to sampling issues, radial strain correlates poorly with reference standards and appears more variable in validation studies [26]. Circumferential and radial strain contributes to overall changes in chamber volume over the cardiac cycle more so than longitudinal strain and thus would better reflect changes in ejection fraction in our model.

Image processing was performed off-line. We used the speckle-tracking algorithm in the EchoPac SW 7.1.1 version PC workstation (GE Medical) in order to measure circumferential strain. Speckle tracking is a method in which ultrasound speckles within the image are tracked and strain is determined from the displacement of speckles in relation to each other, thus making it angle independent. Based on the 2D short-axis images, the end-systole and end-diastole time points were defined; subsequently, three different cardiac cycles from each acquisition were selected for further analysis. Briefly, after selecting the cardiac cycle, the software prompts the operator to apply a region of interest in a "click to point approach" in order to delineate the endocardium. Subsequently the software automatically defines an epicardial and mid-myocardial line and processes all frames of the selected cardiac cycle. Then, the software automatically outlines six segments per short-axis view. The circumferential strain value was calculated for each segment. Circumferential strain values are negative values; as contraction progresses, the circumferential strain values become more negative. Hence, when we refer to circumferential strain values and characterize them as higher in comparison to another value, the higher value is more negative. Segments with poor quality tracking were excluded from the analysis. We calculated the mean circumferential strain which was defined as the average strain of all segments in a particular short-axis view.

Intra-observer and inter-observer variability analyses were performed using five randomly selected studies. For intra-observer analysis, measurements of the five selected studies were repeated on two separate occasions by the same observer. Inter-observer analysis was performed by two independent observers who were blinded to the results of each other.

Statistics

Values are reported as mean±SD. The paired *t* test was used for intra-group comparisons of the various echocardiography measurements in each group at 1 and 4 weeks post-MI. One way ANOVA was used to for the inter-group comparison, while the independent sample *t* test was chosen for the 4 weeks engraftment comparison, comparison of the baseline echocardiography characteristics between the basal and the apical short-axis views and for in vitro studies. A $p<0.05$ was chosen for statistical significance. Mean difference, standard error, upper and lower 95% confidence interval limits, and *t* tests were performed for calculation of inter-observer and intra-observer variability [27].

Results

Confirmation of hHIF-1α Expression in CDCs

Human HIF-1α expression in rat CDCs was confirmed by qPCR. LVCAHif-1α-transduction increased VEGF-A expression by 1.5-fold when compared with control CDCs, under normoxia.

In Vivo Studies

There was no significant difference in LVEF between the three groups of animals, 1 week post-MI indicating that all animals suffered a similar ischemic insult. However, at 4 weeks post-MI, there was no change in left ventricular ejection fraction (EF) in the CELL-HIF group (50.5%±6.8% vs 50.5%±7.4%, $p=0.973$), significant increase in the CELL group (44.6%±7.6% vs 51.5%±7.4%, $p=0.021$,) and significant decrease in the PBS group (47.8% ±4.8% vs 40.2%±4.2%, $p=0.025$) (Fig. 1a).

Intra-observer reproducibility was high for strain (mean difference, 1%; 95% CI, 1.0% to −1.0%). Similarly, no significant differences were noted in inter-observer measurements for strain (mean difference, 1%; 95% CI, 3.0% to −3.0%). We excluded 10% and 14%

segments of the basal SA views (at 1 and 4 weeks post-MI respectively) from strain analysis due to poor tracking quality. There was no significant difference in circumferential strain between the CELL, CELL-HIF, and PBS groups at 7 days following transplantation (mean apical circumferential strain values were −7.3%±1.8%, −7.4%±2.9%, −8.1%±2.0%, p=NS, and the basal mean circumferential strain values were −19.4±2.2, −20.0±2.2, and −19.02.7, respectively.)

In the CELL-HIF group, from weeks 1–4, there was no change in the mean circumferential strain values measured in the infarct/peri-infarct region (−7.4%±2.9% to −7.8%±2.6%, p=NS from apical short-axis views). In contrast, there was a significant increase in this strain parameter in the CELL group (−7.3%±1.8% to −10.4%±1.3%, p=0.019) and a significant decrease in the PBS group (−8.1%±2.0% to −6.6%±1.3%, p=0.024) as shown in Fig. 1b. In all groups of animals, the mean circumferential strain value in the remote basal segments did not change significantly from weeks 1 to 4 post-MI in the PBS group (from −19.0%±2.9% to −17.8±2.4, p=NS), CELL group (from −19.4%±2.2% to −20.0%±1.5%, p=NS) and CELL-HIF group (from −20.0±1.9 to −19.9%±3.6%, p=NS), as illustrated in Fig. 1c.

There was no significant difference in cell engraftment at 1 month between the CELL and the CELL-HIF groups (2.4%±3.3% vs 1.7%±0.8%, p=0.643).

In Vitro Studies

In order to obtain mechanistic insights into our in vivo results, we adopted a reductionist in vitro approach that eliminates the possibility of paracrine crosstalk between CDCs and other cell types present in the heart [28].

Expression Analysis—We examined the effects of hypoxia on endothelin-1 [29], interleukin-1 beta (IL-1β) and VEGF expression [30] in control and HIF-CDCs in vitro. We found that during prolonged hypoxia, which simulates the in vivo infarct environment, expression of endothelin-1 was 2.4-fold higher in LVCAHif-1α-transduced CDCs compared with controls (p=0.001; Fig. 2b); IL-1β was not expressed. VEGF expression increased 13.3-fold in control rCDCs and 14.3-fold in LVCAHif-1α-transduced rCDCs following exposure to hypoxia (Fig. 2a).

Angiogenesis Assay—Within 4 h of plating, both LVCAHif-1α-transduced and control CDCs formed tube-like networks similar to those formed by HUVECs. At 4 and 24 h, there was no significant difference in total tube length (p=0.44) and branch points (p=0.19) between LVCAHif-1α-transduced and control CDCs. Both groups of cells formed closed polygons with sprouting of new tubes (Fig. 2c–f), suggesting that CDCs are angiogenic and rapidly form capillary-like structures in vitro when exposed to endothelial differentiation stimuli.

Proliferation Assay—There was no significant difference in proliferation kinetics between CDCs transduced with LVCAHif-1α and control CDCs, under normoxia and hypoxia, using the WST-8 and EdU incorporation assays (Fig. 2g–i).

Discussion

In this study, we observed that expression of constitutively active HIF-1α in CDCs increased VEGF-A expression, but did not alter angiogenesis potential or proliferation kinetics under normoxia, in vitro. Using echocardiography for assessment of ejection fraction and myocardial strain, a novel, sensitive and well validated indicator of cardiac function [31], we found that transplantation of CDCs stably expressing constitutively active HIF-1α was

superior to PBS injection but inferior to transplantation of non-transduced CDCs (which significantly improved global and regional function 4 weeks post-MI). This result was unexpected based on previous studies of constitutively active HIF-1α in the setting of limb ischemia [5, 6, 15, 32]. In all these studies, injection of an adenovirus expressing the HIF mutant used in this study, into ischemic tissue induced angiogenesis, arteriogenesis, improved tissue perfusion, viability and function by paracrine mechanisms. There are several differences between our study and previous experimental studies using this constitutively active HIF-1α construct [5, 6, 32]. Firstly, we used a lentiviral vector that promotes integration and stable expression of the transgene, in contrast to adenoviral vectors that result in transient (1–2 weeks) expression of the transgene [33]. Secondly, we transduced cells with constitutively active HIF-1α ex vivo, and then injected them intra-myocardially immediately following coronary artery ligation, in contrast to intramuscular injection of adenovirus following vascular occlusion in the hind limb. Based on our data and results from a transgenic mouse model of cardiac HIF-1α over-expression [34], it appears that chronic activation of HIF-1α in the heart may have a deleterious effect on cardiac function. However the mechanisms underlying this effect are not known and need further study.

HIF-1α is a transcription factor that binds hypoxia response elements (HREs) with resultant transcription of >100 genes [35]. One of these genes is endothelin-1 (ET-1) which is a potent vasoconstrictor [36] and has profound effects on cardiac remodeling post-MI by binding to receptors present in cardiac myocytes, fibroblasts and endothelial cells [37, 38]. Previous studies in CDCs reveal that they secrete several factors including VEGF, IGF-1 and HGF that have autocrine and paracrine effects [28, 39]. Since engraftment is low (~50,000 CDCs), paracrine effects of surviving CDCs on tissue preservation and endogeneous regeneration [40] probably played a significant role in determining the functional outcome following transplantation. In fact, a study by Chimenti et al. [39]using CDCs found that direct differentiation of CDCs into endothelial cells and cardiac myocytes could only explain ~20% of the observed benefit.

In this study, we found that endothelin-1 expression was 2.4-fold higher in HIF-CDCs, compared with control CDCs following prolonged exposure to hypoxia, when endogenous HIF expression is expected to be low [12, 13]. Increased secretion of factors like ET-1 by HIF-CDCs in the infarct microenvironment could negate the beneficial effects of other paracrine factors like VEGF and IGF-1, resulting in lack of improvement in myocardial strain of the infarct/peri-infarct region in the HIF-CDC group. Of note, EF and strain in the infarct/peri-infarct region worsened in the PBS group, indicating that HIF expression *blunted* the beneficial effects of CDC therapy.

In our study, lack of benefit from CDCs expressing constitutively active HIF-1α cannot be attributed to a lower proliferation rate since our in vitro studies demonstrated no difference in proliferation or cell viability between LVCAHif-1α-transduced and control CDCs. The in vitro results are confirmed by similar engraftment rates between the CELL and CELL-HIF groups at 4 weeks following CDC transplantation. Additionally, it is unlikely that lack of benefit is mediated by use of a lentiviral vector because we have shown functional benefit in a previous study [2], with this 3rd generation lentiviral vector LvGFP, using the same animal model, multiplicity of infection and operator as in this study.

Limitations

In this study, we examined one constitutively active construct of HIF-1α and one cell type, namely CDCs. Since the effects of HIF activation can vary depending on the cell type and organ system [14, 41], our results need to be confirmed in other stem/progenitor cells.

Additionally, we used in vitro studies under hypoxia to investigate the mechanisms underlying the functional effects of transplantation. The advantage of this study design is that it permits a dissection of the effects of hypoxia and constitutively active HIF-1α expression in CDCs from that on myocytes, fibroblasts, inflammatory and endothelial cells that are present in the infarcted region in this syngeneic model of cell transplantation. Future proteomic studies of the effects of stressors such as hypoxia and metabolic deprivation on paracrine factor secretion by stem/progenitor cells in a different model (xeno-transplantation) are needed to illuminate this issue. Lastly, we did not perform histopathology to investigate the effect of transplantation on cardiomyogenesis, angiogenesis, inflammation, and tissue viability in the infarcted region. Instead, we performed in vitro functional studies, quantified CDC engraftment by qPCR and performed a detailed analysis of regional function which has been shown to correlate well with tissue viability in previous experimental and clinical studies [42]. Lastly, initial echocardiography measurements were performed 1 week post-MI/transplantation, rather than immediately post-MI due to technical difficulties associated with echo imaging in the presence of a left-sided pneumothorax; this study design may have masked early functional benefit in the CDC groups. Nevertheless, we found no difference between the three groups at 1 week and only improvement in the CDC group at 4 weeks, confirming the validity of our results.

Conclusions

Chronic constitutively active HIF-1α expression in CDCs blunted the beneficial functional effects of CDC transplantation, as assessed by echocardiography. Since CDC engraftment is low, this effect is probably due to a HIF-mediated change in paracrine factors like endothelin-1, which can promote adverse remodeling and negate the beneficial influences of factors like VEGF and IGF-1. Our results suggest that paracrine factor balance plays an important role in cell-induced cardiac regeneration.

Acknowledgments

We are grateful to Dr. Farhad Vesuna for help with qPCR, Lee Blosser from the Flow Cytometry Core Analytic Laboratory for help with flow cytometry, Ms. Dana Kemmer for administrative assistance, and Ms. Missy Leppo for helpful advice.

Sources of Funding This study was supported by the WW Smith Foundation (West Conshohocken, PA; MRA), AHA (Dallas, TX; MRA), Maryland TEDCO (Columbia, MD; MRA), NIH RO1 HL092985 (Bethesda, MD; MRA/FB), and GE healthcare (Waukesha, WI).

Abbreviations

CDC	Cardiophere-derived cells
HIF-1α	Hypoxia-inducible factor-1alpha
VEGF	Vascular endothelial growth factor
IL-1β	Interleukin-1 beta IL-1β
ET-1	Endothelin-1
eGFP	Green fluorescent protein
qPCR	Quantitative Polymerase Chain Reaction

References

1. Orlic D, Kajstura J, Chimenti S, Jakoniuk I, Anderson SM, Li B, et al. Bone marrow cells regenerate infarcted myocardium. Nature. 2001; 410(6829):701–705. [PubMed: 11287958]

2. Terrovitis J, Lautamaki R, Bonios M, Fox J, Engles JM, Yu J, et al. Noninvasive quantification and optimization of acute cell retention by in vivo positron emission tomography after intramyocardial cardiac-derived stem cell delivery. Journal of the American College of Cardiology. 2009; 54(17): 1619–1626. doi:10.1016/j.jacc.2009.04.097. [PubMed: 19833262]

3. Bartunek J, Wijns W, Heyndrickx GR, Vanderheyden M. Timing of intracoronary bone-marrow-derived stem cell transplantation after ST-elevation myocardial infarction. Nature Clinical Practice. Cardiovascular Medicine. 2006; 3(Suppl 1):S52–56.

4. Jiang BH, Rue E, Wang GL, Roe R, Semenza GL. Dimerization, DNA binding, and transactivation properties of hypoxia-inducible factor 1. The Journal of Biological Chemistry. 1996; 271(30): 17771–17778. [PubMed: 8663540]

5. Sarkar K, Fox-Talbot K, Steenbergen C, Bosch-Marce M, Semenza GL. Adenoviral transfer of HIF-1alpha enhances vascular responses to critical limb ischemia in diabetic mice. Proceedings of the National Academy of Sciences of the United States of America. 2009; 106(44):18769–18774. [PubMed: 19841279]

6. Rey S, Lee K, Wang CJ, Gupta K, Chen S, McMillan A, et al. Synergistic effect of HIF-1alpha gene therapy and HIF-1-activated bone marrow-derived angiogenic cells in a mouse model of limb ischemia. Proceedings of the National Academy of Sciences of the United States of America. 2009; 106(48):20399–20404. [PubMed: 19948968]

7. Semenza GL. Vascular responses to hypoxia and ischemia. Arteriosclerosis, Thrombosis, and Vascular Biology. 2010; 30(4):648–652.

8. Semenza GL. Regulation of vascularization by hypoxia-inducible factor 1. Annals of the New York Academy of Sciences. 2009; 1177:2–8. [PubMed: 19845601]

9. Rey S, Semenza GL. Hypoxia-inducible factor-1- dependent mechanisms of vascularization and vascular remodelling. Cardiovascular Research. 2010; 86(2):236–242. [PubMed: 20164116]

10. Wang GL, Semenza GL. Characterization of hypoxia-inducible factor 1 and regulation of DNA binding activity by hypoxia. The Journal of Biological Chemistry. 1993; 268(29):21513–21518. [PubMed: 8408001]

11. Semenza GL, Shimoda LA, Prabhakar NR. Regulation of gene expression by HIF-1. Novartis Foundation Symposium. 2006; 272:2–8. discussion 8–14, 33–16. [PubMed: 16686426]

12. Kim CH, Cho YS, Chun YS, Park JW, Kim MS. Early expression of myocardial HIF-1alpha in response to mechanical stresses: regulation by stretch-activated channels and the phosphatidylinositol 3-kinase signaling pathway. Circulation Research. 2002; 90(2):E25–33. [PubMed: 11834720]

13. Lee SH, Wolf PL, Escudero R, Deutsch R, Jamieson SW, Thistlethwaite PA. Early expression of angiogenesis factors in acute myocardial ischemia and infarction. The New England Journal of Medicine. 2000; 342(9):626–633. [PubMed: 10699162]

14. Kelly BD, Hackett SF, Hirota K, Oshima Y, Cai Z, Berg-Dixon S, et al. Cell type-specific regulation of angiogenic growth factor gene expression and induction of angiogenesis in nonischemic tissue by a constitutively active form of hypoxia-inducible factor 1. Circulation Research. 2003; 93(11):1074–1081. [PubMed: 14576200]

15. Patel TH, Kimura H, Weiss CR, Semenza GL, Hofmann LV. Constitutively active HIF-1alpha improves perfusion and arterial remodeling in an endovascular model of limb ischemia. Cardiovascular Research. 2005; 68(1):144–154. [PubMed: 15921668]

16. Sutter CH, Laughner E, Semenza GL. Hypoxia-inducible factor 1alpha protein expression is controlled by oxygen-regulated ubiquitination that is disrupted by deletions and missense mutations. Proceedings of the National Academy of Sciences of the United States of America. 2000; 97(9):4748–4753. [PubMed: 10758161]

17. Yamakawa M, Liu LX, Date T, Belanger AJ, Vincent KA, Akita GY, et al. Hypoxia-inducible factor-1 mediates activation of cultured vascular endothelial cells by inducing multiple angiogenic factors. Circulation Research. 2003; 93(7):664–673. [PubMed: 12958144]

18. Kizana E, Chang CY, Cingolani E, Ramirez-Correa GA, Sekar RB, Abraham MR, et al. Gene transfer of connexin43 mutants attenuates coupling in cardiomyocytes: novel basis for modulation of cardiac conduction by gene therapy. Circulation Research. 2007; 100(11):1597–1604. [PubMed: 17495226]

19. Yingzhong Y, Fan W, Zhu L, Zhao T, Ma L, Wu Y, et al. Effects of hypoxia on mRNA expression of housekeeping genes in rat brain tissue and primary cultured neural cells. Fronteirs of Medicine in China. 2008; 2:239–243.
20. Chen J, He L, Dinger B, Stensaas L, Fidone S. Role of endothelin and endothelin A-type receptor in adaptation of the carotid body to chronic hypoxia. American Journal of Physiology. Lung Cellular and Molecular Physiology. 2002; 282(6):L1314–1323. [PubMed: 12003788]
21. Fukushima S, Varela-Carver A, Coppen SR, Yamahara K, Felkin LE, Lee J, et al. Direct intramyocardial but not intracoronary injection of bone marrow cells induces ventricular arrhythmias in a rat chronic ischemic heart failure model. Circulation. 2007; 115(17):2254–2261. [PubMed: 17438152]
22. Berridge MV, Herst PM, Tan AS. Tetrazolium dyes as tools in cell biology: new insights into their cellular reduction. Biotechnology Annual Review. 2005; 11:127–152.
23. Abraham TP, Laskowski C, Zhan WZ, Belohlavek M, Martin EA, Greenleaf JF, et al. Myocardial contractility by strain echocardiography: comparison with physiological measurements in an in vitro model. American Journal of Physiology. Heart and Circulatory Physiology. 2003; 285(6):H2599–2604. doi:10.1152/ajpheart.00994.2002. [PubMed: 12907429]
24. Urheim S, Cauduro S, Frantz R, McGoon M, Belohlavek M, Green T, et al. Relation of tissue displacement and strain to invasively determined right ventricular stroke volume. The American Journal of Cardiology. 2005; 96(8):1173–1178. doi:10.1016/j.amjcard.2005.06.049. [PubMed: 16214459]
25. Helm RH, Leclercq C, Faris OP, Ozturk C, McVeigh E, Lardo AC, et al. Cardiac dyssynchrony analysis using circumferential versus longitudinal strain: implications for assessing cardiac resynchronization. Circulation. 2005; 111(21):2760–2767. doi:10.1161/CIRCULATIONAHA.104.508457. [PubMed: 15911694]
26. Langeland S, D'Hooge J, Wouters PF, Leather HA, Claus P, Bijnens B, et al. Experimental validation of a new ultrasound method for the simultaneous assessment of radial and longitudinal myocardial deformation independent of insonation angle. Circulation. 2005; 112(14):2157–2162. doi:10.1161/CIRCULATIONAHA.105.554006. [PubMed: 16203928]
27. Koopman LP, Slorach C, Hui W, Manlhiot C, McCrindle BW, Friedberg MK, et al. Comparison between different speckle tracking and color tissue Doppler techniques to measure global and regional myocardial deformation in children. Journal of the American Society of Echocardiography. 2010; 23(9):919–928. doi:10.1016/j.echo.2010.06.014. [PubMed: 20655173]
28. Stastna M, Chimenti I, Marban E, Van Eyk JE. Identification and functionality of proteomes secreted by rat cardiac stem cells and neonatal cardiomyocytes. Proteomics. 2010; 10(2):245–253. [PubMed: 20014349]
29. Belaidi E, Joyeux-Faure M, Ribuot C, Launois SH, Levy P, Godin-Ribuot D. Major role for hypoxia inducible factor-1 and the endothelin system in promoting myocardial infarction and hypertension in an animal model of obstructive sleep apnea. Journal of the American College of Cardiology. 2009; 53(15):1309–1317. [PubMed: 19358946]
30. Watson JA, Watson CJ, McCrohan AM, Woodfine K, Tosetto M, McDaid J, et al. Generation of an epigenetic signature by chronic hypoxia in prostate cells. Human Molecular Genetics. 2009; 18(19):3594–3604. [PubMed: 19584087]
31. Dandel M, Lehmkuhl H, Knosalla C, Suramelashvili N, Hetzer R. Strain and strain rate imaging by echocardiography—basic concepts and clinical applicability. Current Cardiology Review. 2009; 5(2):133–148.
32. Bosch-Marce M, Okuyama H, Wesley JB, Sarkar K, Kimura H, Liu YV, et al. Effects of aging and hypoxia-inducible factor-1 activity on angiogenic cell mobilization and recovery of perfusion after limb ischemia. Circulation Research. 2007; 101(12):1310–1318. [PubMed: 17932327]
33. Barth AS, Kizana E, Smith RR, Terrovitis J, Dong P, Leppo MK, et al. Lentiviral vectors bearing the cardiac promoter of the Na+–Ca2+ exchanger report cardiogenic differentiation in stem cells. Molecular Therapy. 2008; 16(5):957–964. [PubMed: 18388932]
34. Lei L, Mason S, Liu D, Huang Y, Marks C, Hickey R, et al. Hypoxia-inducible factor-dependent degeneration, failure, and malignant transformation of the heart in the absence of the von Hippel–Lindau protein. Molecular and Cellular Biology. 2008; 28(11):3790–3803. [PubMed: 18285456]

35. Ke Q, Costa M. Hypoxia-inducible factor-1 (HIF-1). Molecular Pharmacology. 2006; 70(5):1469–1480. [PubMed: 16887934]

36. Yanagisawa M, Kurihara H, Kimura S, Tomobe Y, Kobayashi M, Mitsui Y, et al. A novel potent vasoconstrictor peptide produced by vascular endothelial cells. Nature. 1988; 332(6163):411–415. [PubMed: 2451132]

37. Hocher B, George I, Rebstock J, Bauch A, Schwarz A, Neumayer HH, et al. Endothelin system-dependent cardiac remodeling in renovascular hypertension. Hypertension. 1999; 33(3):816–822. [PubMed: 10082493]

38. Rebsamen MC, Church DJ, Morabito D, Vallotton MB, Lang U. Role of cAMP and calcium influx in endothelin-1-induced ANP release in rat cardiomyocytes. The American Journal of Physiology. 1997; 273(5 Pt 1):E922–931. [PubMed: 9374678]

39. Chimenti I, Smith RR, Li TS, Gerstenblith G, Messina E, Giacomello A, et al. Relative roles of direct regeneration versus paracrine effects of human cardiosphere-derived cells transplanted into infarcted mice. Circulation Research. 2010; 106(5):971–980. [PubMed: 20110532]

40. Gnecchi M, Zhang Z, Ni A, Dzau VJ. Paracrine mechanisms in adult stem cell signaling and therapy. Circulation Research. 2008; 103(11):1204–1219. [PubMed: 19028920]

41. Semenza GL. Hydroxylation of HIF-1: oxygen sensing at the molecular level. Physiology (Bethesda). 2004; 19:176–182. [PubMed: 15304631]

42. Popovic ZB, Benejam C, Bian J, Mal N, Drinko J, Lee K, et al. Speckle-tracking echocardiography correctly identifies segmental left ventricular dysfunction induced by scarring in a rat model of myocardial infarction. The American Journal of Physiology. 2007; 292(6):H2809–2816.

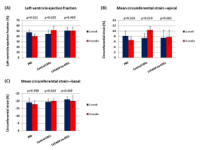

Fig. 1.

Constitutively active HIF-1α transduction blunted the beneficial effects of CDC transplantation on cardiac function 4 weeks post-MI. **a** Left ventricular ejection fraction was unchanged in the CELL-HIF group, improved in the CELL group and worsened in the PBS group. **b** Mean circumferential strain obtained from the apical short-axis views was unchanged in the CELL-HIF group, improved in the CELL group and worsened in the PBS group. **c** Mean circumferential strain values measured in the basal short-axis views (non-infarcted and remote myocardial region) at 1 and 4 weeks post-MI in the PBS, CELL, and CELL-HIF groups were similar

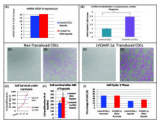

Fig. 2.

Effects of constitutively active HIF-1α on CDC physiology and angiogenic potential. **a** VEGF expression increased 13.3-fold in control rCDCs and 14.3-fold in LVCAHif-1α-transduced rCDCs following exposure to hypoxia in vitro. **b** Endothelin-1 mRNA expression was 2.4-fold higher in HIF-CDCs than control CDCs during prolonged hypoxia in vitro. **c**–**f** Representative images of tube formation by control (**c**) and LVCAHif-1α-transduced rCDCs (**e**) and their corresponding images after tracing (*pink lines*) to measure total tube length after 24 h of culture (**d** and **f**). There was no significant difference in total tube length and branch points between the two groups. **g** LVCAHif-1α expression did not affect proliferation kinetics of CDCs under normoxia or after 48 h of hypoxia (**h**), when assessed by the WST-8 assay. **i** There was no significant difference between the percentage of LVCAHif-1α-transduced and control CDCs entering the S phase of the cell cycle when assessed by flow cytometry using Edu and 7AAD